

SUPERSATURATIONS IN CIRRUS: FIELD AND LABORATORY OBSERVATIONS

M. Krämer¹, C. Schiller¹, A. Afchine¹, R. Bauer¹,
I. Gensch¹, A. Mangold^{1,7}, S. Schlicht¹, N. Spelten¹,
O. Möhler², H. Saathoff², V. Ebert³, N. Sitnikov⁴,
M. de Reus⁵, S. Borrmann⁵ and P. Spichtinger⁶

¹ Research Center Jülich, Germany, ² Research Center Karlsruhe, Germany,
³ University Heidelberg, Germany, ⁴ Central Aerological Observatory, Moscow Region,
Russia, ⁵ University Mainz, Germany, ⁶ ETH Zürich, Switzerland,
⁷ Royal Meteorological Institute, Bruxelles, Belgium

1. OVERVIEW

Upper tropospheric water vapor supersaturations over ice of up to unexplained 200% inside and outside of cold cirrus clouds are frequently reported from aircraft and balloons in recent years (Ovarlez et al. (2002), Gao et al. (2004), Jensen et al. (2005), Vömel and David (2007)). Such supersaturations may have significant impact on climate, since higher critical supersaturation for ice cloud formation than hitherto assumed will lead to a decrease in high cloud cover, which in turn feeds back to the radiation balance of the atmosphere Gettelman and Kinnison (2007). Supersaturations inside cirrus interact with the ice clouds microphysics and thus with the radiative properties of the cloud as well as the vertical redistribution of water vapor through sedimentation of ice crystals. Peter et al. (2006) summarised this 'supersaturation puzzle' and raise the question whether it maybe caused by a lack of understanding of conventional ice cloud microphysics or by uncertainties or flaws in the water instruments.

Here, we present high quality field observations of supersaturations in and outside of cirrus from 28 flights in ten field campaigns in Arctic, mid-latitude and tropical cirrus clouds. In our data set, no supersaturations larger than 200% are found.

In addition, the temporal evolution of supersaturations in ice clouds formed at the aerosol chamber AIDA by different types of aerosol particles are shown. Combined analysis of the field as well as the laboratory observations suggests that conventional ice cloud microphysics can explain our supersaturation observations.

2. EXPERIMENTALS

Water vapor measurements from several instruments operated on three different aircraft and in the AIDA chamber during the above mentioned campaigns are analyzed in the present study.

During field experiments with the Russian M55 Geophysica, water vapor was determined simultaneously with the FISH (Fast In-situ Stratospheric Hygrometer) and the FLASH (FLuorescent Airborne Stratospheric Hygrometer), both closed cell Lyman- α fluorescence hygrometers. The FISH is equipped with a forward facing inlet sampling total water, i.e. gas phase + ice water. Ice particles are over-sampled with an enhancement depending on altitude and cruising speed of the aircraft. Corrections are applied during post-flight analysis. The FLASH uses a down-ward facing inlet that excludes ice particles and samples only gas phase water. Those experiments that used the German *enviscope*-Learjet or DLR Falcon em-

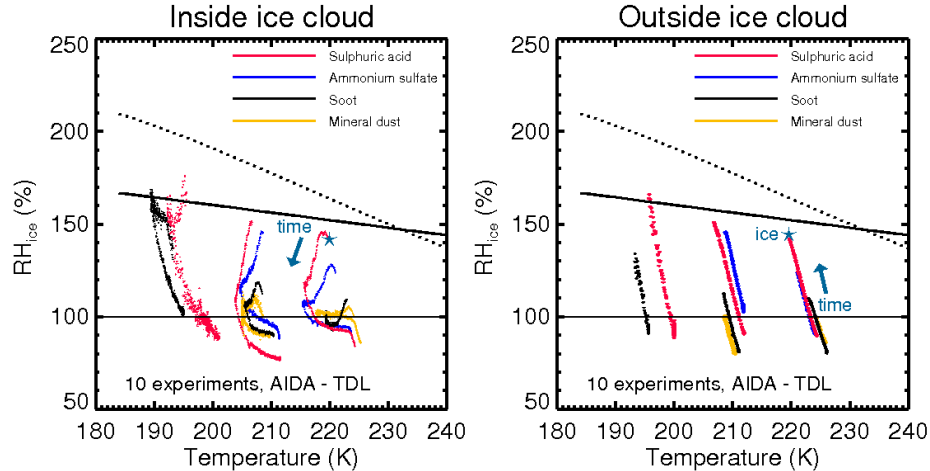


Figure 1: AIDA laboratory observations of RH_{ice} vs. temperature in- and outside of cirrus for 10 ice nucleation experiments initiated by different aerosol particles. The arrow shows the direction of time of the experiments, the star denotes for one exemplary experiment the point where ice crystals appear for the first time. The black dotted line represents water saturation, the black solid line the homogeneous freezing threshold after Koop et al. (2000).

ployed versions of the FISH for the total water measurements, while gas phase water was measured with the open path TDL OJSTER (Open path Juelich Stratospheric Tdl ExpeRiment, MayComm Instruments). During laboratory campaigns at the AIDA chamber, gas phase water was also measured with an open path TDL.

The relative humidity with respect to ice, RH_{ice} , is calculated as $(H_2O_{gas}/H_2O_{sat,ice}) \cdot 100$ (H_2O_{gas} : gas phase water vapor, $H_2O_{sat,ice}$: water vapor saturation wrt ice after Marti and Mauersberger (1993)). The term 'supersaturation' refers to relative humidities with respect to that ice that exceeds 100%.

3. AIDA ICE NUCLEATION EXPERIMENTS

The ice nucleation experiments performed at the AIDA chamber offer the possibility to study the RH_{ice} evolution in cirrus life cycles (operation of the AIDA facility as an expansion cloud chamber for ice nucleation studies is described in detail by Möhler et al. (2003) or Mangold et al. (2005)).

RH_{ice} inside and outside of ice clouds generated at the AIDA chamber are shown in Fig-

ure 1 for ten ice nucleation experiments initiated by different aerosol particles. As homogeneously freezing aerosol sulfuric acid - water (red) and ammonium sulfate (blue) particles were injected in the AIDA chamber. In addition, as heterogeneously freezing particle types soot (black) and mineral dust (yellow) were used. These particle types are chosen because they are believed to be important components of the upper tropospheric aerosol particle population, though the knowledge of the aerosol in this altitude is very limited.

3.1 Outside AIDA ice clouds

In Figure 1 (right panel) RH_{ice} before ice formation is shown for aerosol particles with differing freezing thresholds. Each stroke represents one experiment and the freezing thresholds are the upper ends of the strokes (the star denotes for one exemplary experiment the point where ice crystals appear for the first time).

During the homogeneous ice nucleation experiments with liquid sulfuric acid-water particles (red strokes) RH_{ice} increases up to around the homogeneous freezing threshold derived by Koop et al. (2000) (black solid line). Ammo-

nium sulfate particles (blue), though liquid, nucleate below the homogeneous freezing threshold, because crystallization in the liquid droplets already starts during the cooling process (Mangold et al., 2005). Soot and mineral dust particles (black and yellow) freeze well below the homogeneous freezing threshold, mineral dust already at RH_{ice} only slightly exceeding 100% (Mangold et al. (2005), Möhler et al. (2005)). In addition to the dependence of the freezing thresholds on the aerosol type, it can be seen that ice nucleation occurs at higher supersaturations for lower temperatures.

3.2 Inside AIDA ice clouds

In the left panel of Figure 1 RH_{ice} after ice formation is shown for the same experiments as in the right panel, i.e. the coloured curves in the left panel continue the respective right panels strokes. Note here that the RH_{ice} development inside of the AIDA ice clouds is not directly comparable to the atmosphere because of the H_2O flux from the wall into the chamber during the existence of ice crystals. However, a qualitative picture of the evolution of RH_{ice} during an ice cloud cycle can be derived from the AIDA observations.

After ice crystal formation and continuous cooling RH_{ice} still rises up to a 'peak RH_{ice} '. This increase in RH_{ice} is because the ice crystals are so small in the beginning, that the water depletion of the gas phase is not large enough to compensate the increase of RH_{ice} caused by the further cooling. Consequently, the duration and the degree of the post-ice RH_{ice} increase depend on the number of ice crystals formed during the nucleation. A lower number of ice crystals appear for heterogeneously formed ice clouds. Thus, the few ice crystals consume the water vapour much slower and therefore RH_{ice} raises until a plateau after ice formation (see for example the yellow mineral dust experiments). In colder ice clouds, this behaviour becomes more pronounced and appears also for homogeneously forming ice clouds (see red and black experiments for sulfuric acid and soot, respectively). For the homogeneous sul-

furic acid-water experiment (red) at the lowest temperature (<200 K), it can be seen that after the ice nucleation at the homogeneous threshold RH_{ice} even shortly exceeds the homogeneous freezing line.

When cooling is stopped (the experiment curves turn to the right to higher temperatures), RH_{ice} immediately drops very quickly down to saturation and below, while ice crystals still exist. The part of the cirrus cycle where the crystals are evaporating is represented by the sub-saturated part of the in-cloud observations.

4. CIRRUS FIELD OBSERVATIONS

4.1 Clear sky

Frequencies of occurrence of RH_{ice} outside of cirrus in dependence on temperature are plotted in Figure 2 (top panel). From our clear sky observations, representing about 16 hours of aircraft flight time, it can be seen that RH_{ice} between nearly zero up to the homogeneous freezing thresholds are possible for temperatures >200 K. For lower temperatures, the highest frequencies of occurrence of RH_{ice} is enveloped by the dashed lines, representing RH_{ice} in dependence of temperature for a constant value of 2 and 3 ppmv, corresponding to the range of water vapour mixing ratios observed in the upper troposphere.

Although the AIDA experiments do not cover the complete temperature range observed during the field observations and more laboratory studies would be desirable, the general picture of the AIDA cloud free supersaturations matches that of the clear sky supersaturations observed in the upper troposphere.

No supersaturations close to or above water saturation are observed in our field measurements. Thus, from our data set we could not confirm the hypothesis of suppression of ice cloud formation.

4.2 In - cloud

The frequencies of occurrence of in-cloud RH_{ice} observed in the field (Figure 2, bottom panel)

show a pattern comparable to the AIDA measurements. Above about 200 K, values of RH_{ice} between around 50% and the homogeneous freezing thresholds are found, but most of the RH_{ice} observations group around 100%. Less frequent high supersaturations are probably observed in young cirrus directly after ice formation, while subsaturations are from old cirrus in the evaporation stage. This is a hint to short water vapour relaxation times in this temperature range, causing these parts of the clouds life cycle to be short compared to the time the clouds live around saturation.

At temperatures lower than about 200K, the grouping of the RH_{ice} frequencies of occurrence around saturation broadens, pointing to longer water vapour relaxation times as for the warmer cirrus. There is no clear supersaturation cycle during the cirrus lifetime in this temperature range, as also seen from the AIDA experiments shown in Figure 1 (left panel).

No supersaturations above water saturation are observed in our field measurements, but, in the low temperature range, we observed few data points between the homogeneous freezing threshold and water saturation. By comparison with the AIDA observations, these measurements could be interpreted as the very first part of the cirrus life cycle, where RH_{ice} is between the freezing threshold and the 'peak RH_{ice} '.

REFERENCES

- Gao, R., Popp, P., Fahey, D., Marcy, T., Herman, R., Weinstock, E., Baumgardener, D., Garrett, T., Rosenlof, K., Thompson, T., Bui, P., Ridley, B., Wofsy, S., Toon, B., Tolbert, M., Kärcher, B., Peter, T., Hudson, P., Weinheimer, A., and Heymsfield, A.: Evidence That Nitric Acid Increases Relative Humidity in Low-Temperature Cirrus Clouds, *Science*, 303, 516 – 520, 2004.
- Gottelman, A. and Kinnison, D. E.: The global impact of supersaturation in a coupled chemistry-climate model, *Atmos. Chem. Phys.*, 7, 1629–1643, 2007.
- Jensen, E., Smith, J., Pfister, L., Pittman, J., Weinstock, E., Sayres, D., Herman, R., Troy, R., Rosenlof, K., Thompson, T., Fridlind, A., Hudson, P., Cziczo, D., Heymsfield, A., Schmitt, C., and Wilson, J.: Ice supersaturations exceeding 100% at the cold tropical tropopause: implications for cirrus formation and dehydration, *Atmos. Chem. Phys.*, 5, 851–862, 2005.
- Koop, T., Luo, B., Tsias, A., and Peter, T.: Water activity as the determinant for homogeneous ice nucleation in aqueous solutions, *Nature*, 406, 611 – 614, 2000.
- Mangold, A., Wagner, R., Saathoff, H., Schurath, U., Giesemann, C., Ebert, V., Krämer, M., and Möhler, O.: Experimental investigation of ice nucleation by different types of aerosols in the aerosol chamber AIDA: implications to microphysics of cirrus clouds, *Meteorol. Z.*, 14, 485 – 497, 2005.
- Marti, J. and Mauersberger, K.: A survey and new measurements of ice vapor pressure at temperatures between 170K and 250K, *Geophys. Res. Lett.*, 20, 363–366, 1993.
- Möhler, O., Stetzer, O., Schaefers, S., Linke, C., Schnaiter, M., Tiede, R., Saathoff, H., Krämer, M., Mangold, A., Budz, P., Zink, P., Schreiner, J., Mauersberger, K., Haag, W., Kärcher, B., and Schurath, U.: Experimental investigation of homogeneous freezing of sulphuric acid particles in the aerosol chamber AIDA, *Atmos. Chem. Phys.*, 3, 211–223, 2003.
- Möhler, O., Büttner, S., Linke, C., Schnaiter, M., Saathoff, H., Stetzer, O., Wagner, R., Krämer, M., Mangold, A., Ebert, V., and Schurath, U.: Effect of sulfuric acid coating on heterogeneous ice nucleation by soot aerosol particles, *J. Geophys. Res.*, 110, 2005.
- Ovarlez, J., Gayet, J.-F., Gierens, K., Ström, J., Ovarlez, H., Auriol, F., Busen, R., and Schumann, U.: Water vapour measurements inside cirrus clouds in Northern and Southern hemispheres during INCA, *Geophys. Res. Lett.*, 29, 1813, doi: 10.1029/2001GL014440, 2002.
- Peter, T., Marcolli, C., Spichtinger, P., Corti, T., Baker, M., and Koop, T.: When dry air is too humid, *Science*, 314, 1399 – 1401, 2006.
- Vömel, H. and David, D.E. and Smith, K.: Accuracy of tropospheric and stratospheric water vapor measurements by the cryogenic frost point hygrometer: Instrumental details and observations, *J. Geophys. Res.*, 112, doi: 10.1029/2006JD007224, 2007.

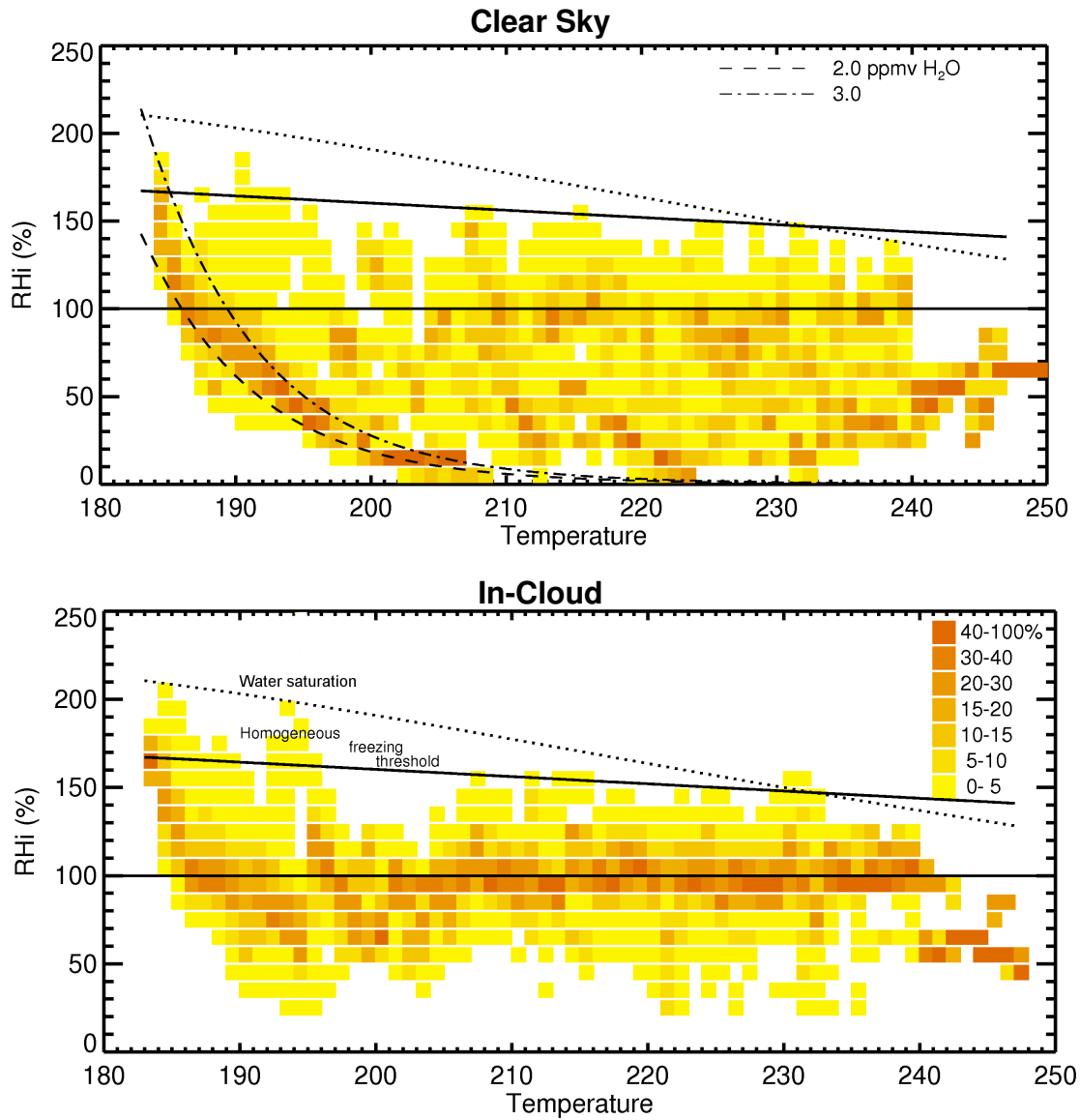


Figure 2: Frequencies of occurrence of supersaturations vs. temperature, observed during 28 flights in Arctic, mid-latitude and tropical cirrus (data are sorted in 1K temperature bins; solid line: homogeneous freezing threshold, dotted line: water saturation line). **Top panel:** Outside of cirrus (16 h flight time); dashed lines: RH_{ice} calculated for constant water vapor mixing ratios of 2 and 3 ppmv, respectively. **Bottom panel:** Inside of cirrus (13 h flight time).